

Dynamic Properties of a Two-Dimensional Heisenberg Antiferromagnet at Low Temperatures

Stéphane Tyč and Bertrand I. Halperin

Jefferson Laboratory of Physics, Harvard University, Cambridge, Massachusetts 02138

Sudip Chakravarty^(a)

Department of Physics, State University of New York at Stony Brook, Stony Brook, New York 11794-3800

(Received 19 December 1988)

By using a combination of hydrodynamics, scaling, and renormalization-group analysis, and a fit to the simulations of a *classical* rotor model, we can predict the form of the dynamic structure factor $S(\mathbf{k}, \omega)$ of a two-dimensional quantum Heisenberg antiferromagnet at low temperatures, if the zero-temperature spin-stiffness constant ρ_s and magnetic susceptibility χ_\perp^0 are known. These results should be applicable to inelastic neutron scattering in stoichiometric La_2CuO_4 above its Néel temperature, with only ρ_s as an adjustable parameter.

PACS numbers: 75.25.+z, 74.65.+n, 75.10.Jm, 75.30.-m

The discovery of high-temperature superconductors has led to a renewed interest in quantum antiferromagnets. Recently, Endoh *et al.*¹ have made neutron-diffraction experiments on the stoichiometric insulating phase of La_2CuO_4 and have observed strong antiferromagnetic correlations in the plane of the copper atoms above the Néel temperature T_N where three-dimensional order sets in. Chakravarty, Halperin, and Nelson² (CHN) have argued that these measurements could be understood in terms of a nearest-neighbor two-dimensional quantum Heisenberg antiferromagnet (QHAF) on a square lattice with spin $S = \frac{1}{2}$ and a large coupling constant J of order 1200 K.

CHN argue that the dynamic properties of the QHAF at sufficiently low temperatures and frequencies, and wave vectors close to the antiferromagnetic Bragg peak, may be related directly to the low-frequency long-wavelength behavior of a *classical* lattice rotor model (CLRM) [defined by Eq. (13) below], which can be studied by molecular-dynamics simulations. The relations between the QHAF and CLRM were established by a combination of hydrodynamics, scaling, and a renormalization-group analysis in which it was necessary to include terms up to "two-loop order." There are no adjustable parameters in this correspondence provided that the *zero-temperature* properties of the QHAF are known (specifically the spin-stiffness constant ρ_s and the uniform magnetic susceptibility χ_\perp^0 for magnetic fields perpendicular to the sublattice magnetization are required). In applications to a physical system such as La_2CuO_4 , where the microscopic coupling constant is not known, it is convenient to use ρ_s as an adjustable parameter which sets the energy scale of the system; the remaining parameters are then determined with an accuracy sufficient for our purposes via a simple spin-wave expansion for the nearest-neighbor spin- $\frac{1}{2}$ Heisenberg model on a square lattice at $T=0$.³

In this paper we present a molecular-dynamics simulation of the CLRM which tests the scaling forms of CHN and determines the previously unknown scaling func-

tions. We are therefore able to give a *quantitative* prediction for the QHAF that can be compared in the future to inelastic-neutron-scattering experiments in La_2CuO_4 . We simulate lattices of size up to 256×256 and thus we can probe temperatures lower than has been done so far. We reproduce the results for the static order-parameter correlation function $S(\mathbf{k})$ with improved accuracy, and we find that the dynamical correlation function $S(\mathbf{k}, \omega)$ is described very well by the scaling forms of CHN. The location of the spin-wave peaks agrees with the approximate CHN prediction and the order-parameter relaxation rate at $k=0$ is in good agreement with the value obtained by Grepel from a coupled-mode calculation.⁴ (Note, in applications to the *spin* correlation function measured by neutron scattering in La_2CuO_4 , the wave vector \mathbf{k} must be interpreted as the distance from the 2D antiferromagnetic Bragg point.)

According to CHN, the dynamic order-parameter correlation function $S(\mathbf{k}, \omega)$ at wave vector \mathbf{k} and frequency ω , for either the QHAF or the CLRM, *in the scaling regime*, can be written in the form

$$S(k, \omega) = \bar{\omega}_0^{-1} S(k) \Phi(q, \nu), \quad (1)$$

$$\bar{\omega}_0 \equiv c \xi^{-1} (T/2\pi\rho_s)^{1/2}, \quad (2)$$

where $S(k)$ is the equal-time correlation function, ξ is the order-parameter correlation length at temperature T , c is the *zero-temperature* long-wavelength spin-wave velocity, given by $c = (\rho_s/\chi_\perp^0)^{1/2}$, and the scaling variables are $\nu \equiv \omega/\bar{\omega}_0$ and $q \equiv k\xi$.

The equilibrium statistical properties of the CLRM are identical to those of the classical Heisenberg ferromagnet. According to the two-loop renormalization-group analysis, the correlation length for these models may be written in the asymptotic form

$$\xi = B_\xi b \frac{\exp(2\pi\rho_s/T)}{(2\pi\rho_s/T) + 1}, \quad (3)$$

where b is the lattice constant and B_ξ is a dimensionless

constant. The value of B_ξ was originally determined by Shenker and Tobochnik⁵ via Monte Carlo simulations to be $B_\xi^{ST} \approx 0.01$, and we obtain the same result. The second term in the denominator of (3), which is small compared to the leading term in the limit $T \rightarrow 0$, is not a result of the renormalization-group analysis but is only a plausible correction term introduced by Shenker and Tobochnik to improve the accuracy of fits at finite values of T . We follow their suggestion, and also include similar corrections in Eqs. (5) and (7) below.

According to CHN, the transformation from the CLRM to the QHAF can be implemented by replacing the lattice constant b , in (3), by the temperature-dependent quantity

$$b_{\text{eff}} = \sqrt{32} e^{\pi/2} (\hbar c/T), \quad (4)$$

which means that for a QHAF with lattice constant a ,

$$\xi = C_\xi a \frac{\exp(2\pi\rho_s/T)}{1 + (T/2\pi\rho_s)}. \quad (5)$$

Using the results of Oguchi³ for the zero-temperature properties of the nearest-neighbor QHAF on a square lattice, CHN find $C_\xi \approx 0.5$, for $S = \frac{1}{2}$.

According to the renormalization-group analysis, the equal-time correlation function $S(k)$ has the scaling form

$$S(k) = S(k=0) f(k\xi), \quad (6)$$

$$S(k=0) = \frac{B_S \xi^2 N_0^2}{[(2\pi\rho_s/T) + 1]^2}, \quad (7)$$

where B_S is a universal constant, and N_0 is the value of the order parameter at $T=0$. For the CLRM, we have $N_0=1$, while for the $S = \frac{1}{2}$ QHAF, we have $N_0 \approx 0.31$. Our normalization is such that for high temperatures, $S(k) = b^2$ for the CLRM and $S(k) = a^2 S(S+1)$ for the QHAF. The Monte Carlo results of Shenker and Tobochnik imply $B_S \approx 180$; we find $B_S \approx 125$.

A one-parameter approximate form for the scaling function f is

$$f(x) \approx \frac{1 + \frac{1}{2} B_f \ln(1+x^2)}{1+x^2}. \quad (8)$$

In the limit $T \rightarrow 0$, with $k\xi \rightarrow \infty$ but $kb_{\text{eff}} \ll 1$, we must have $S(k) \sim 2TN_0^2/\rho_s k^2$. This implies the relation

$$B_S B_f = 4\pi. \quad (9)$$

Our molecular-dynamics results were fitted with a two-Lorentzian form for the dynamic scaling function:

$$\Phi(q, \nu) \approx \frac{\gamma_q}{(\nu - \nu_q)^2 + \gamma_q^2} + \frac{\gamma_q}{(\nu + \nu_q)^2 + \gamma_q^2}, \quad (10)$$

while the dimensionless spin-wave frequency ν_q and the

width γ_q were fitted with the expressions

$$\nu_q = \left(\frac{3}{2}\right)^{1/2} q [\delta + \frac{1}{2} \ln(1+q^2)]^{1/2}, \quad (11)$$

$$\gamma_q = \frac{\gamma_0 (1 + \mu q^2)^{1/2}}{[1 + \frac{1}{2} \theta \ln(1+q^2)]^{w-1/2}}, \quad (12)$$

with the exponent $w=2$, and four adjustable fitting parameters, γ_0 , μ , θ , and δ . The choice of these expressions was influenced by the following considerations: (i) According to the hydrodynamic analysis of CHN, the spin-wave frequency must satisfy $\nu_q \sim (\frac{3}{2})^{1/2} q \ln q$, for $q \rightarrow \infty$. (ii) For large values of q , we believe the width of the spin-wave peak should be dominated by scattering from a thermally excited spin wave with wave vector k' such that $k'\xi$ is comparable to q . A self-consistent analysis, whose details will be given elsewhere, suggests that for large q , $\gamma_q/\nu_q \sim \text{const} \times (\ln \ln q)/(\ln q)^2$.⁶ Equation (12) agrees with this form for $q \rightarrow \infty$ if we ignore the slowly varying factor $\ln \ln q$. (iii) Our molecular-dynamics simulations were fitted very adequately by a single Lorentzian at $q=0$; hence it was appropriate to choose a form where $\nu_q \rightarrow 0$ for $q \rightarrow 0$. Attempts to fit with a form which allowed $\nu_0 \neq 0$ led to a value of ν_0 which was not distinguishable from zero. (iv) Equations (10)–(12) give a form for $\Phi(\nu, q)$ which is analytic in q , for $q \rightarrow 0$.

We shall now discuss in greater detail the method of simulation of the CLRM and the results we obtained. The model is described by a classical Lagrangian of the form

$$L = \frac{I}{2} \sum_i |\dot{\mathbf{n}}_i|^2 + \frac{K}{b^2} \sum_{\langle i,j \rangle} \mathbf{n}_i \cdot \mathbf{n}_j, \quad (13)$$

where $\{\mathbf{n}_i\}$ are a set of three-dimensional unit vectors, representing the orientations of the rotors associated with the sites $\{i\}$ of a 2D square lattice, and the second sum is over nearest-neighbor pairs $\langle i,j \rangle$. The coefficient K is a stiffness constant which we may identify with the constant ρ_s , while the moment of inertia I of the rotors is related to χ_\perp^0 by $\chi_\perp^0 \equiv Ib^2$. Each site represents a rotor which can be thought of as a point mass constrained to stay on the surface of a unit three-dimensional sphere. The interaction between neighbors is such that they want to be aligned. We simulate the dynamics at finite temperature of a $N \times N$ square lattice of rotors, with $N=256$ for the low temperatures.

In order to obtain a canonical ensemble, we couple the system to a heat bath, which introduces a random force and a damping on each rotor. The equations of motion are then Langevin equations:

$$\mathbf{n}_i \times \ddot{\mathbf{n}}_i = -\frac{K}{Ib^2} \mathbf{n}_i \times \sum_j' (\mathbf{n}_i - \mathbf{n}_j) - \gamma \mathbf{n}_i \times \dot{\mathbf{n}}_i + \mathbf{n}_i \times \boldsymbol{\eta}_i(t), \quad (14)$$

where γ is the coupling constant to the heat bath, the sum is restricted to nearest-neighbors of i , and the ran-

dom force η_i obeys

$$\langle \eta_i^\alpha(t) \eta_j^\beta(t') \rangle = 2\gamma k_B T \delta_{ij} \delta(t-t') \delta_{\alpha\beta}. \quad (15)$$

We use units such that $K=1$, $I=1$, and $b=1$. At the beginning of the program the rotors start from a random position with zero initial velocity and are strongly coupled to the heat bath ($\gamma=1$) for 1200 iterations. This is long enough to bring the measured temperature \bar{T} ($\bar{T} \equiv N^{-2} E_{\text{kinetic}}$) to within 1% of the input temperature T . We then reduce the damping to $\gamma=0.00625$ for our actual runs. The nonzero γ is used to assure that there is no secular drift in the temperature, and also to assure that the system is not trapped in one region of phase space. In fitting our formulas, we have corrected for the finite external damping by including a term $0.00625/\bar{\omega}_0$ on the right-hand side of Eq. (11).

The correlation functions $S(k, \omega)$ are calculated for a run which corresponds to 2^{15} time steps. At the end of a run, a configuration of the system is preserved and is then used as the seed of the next run. At equilibrium, positions and velocities are independent; hence a new thermalized sample is obtained by starting from the positions at the end of the previous run and giving the rotors a set of new velocities according to a two-dimensional Maxwellian distribution at the given temperature. At each temperature a number of runs (at least six) are made and the quantities of interest are averaged.

The discretized equations of motion are a modified version of the algorithm used by Morf and Stoll⁷:

$$\begin{aligned} \mathbf{\Omega}(t+\Delta) = \mathbf{\Omega}_0(t+\Delta) + (e^{-\gamma\Delta} - 1)[\mathbf{\Omega}_0(t+\Delta) - \mathbf{\Omega}(t)] \\ - \Delta^2 e^{(-\gamma\Delta/2)} \bar{\mathbf{F}}(t) + O(\Delta^4), \quad (16) \end{aligned}$$

where $\mathbf{\Omega}_0(t+\Delta)$ is the position the rotor would have at time $t+\Delta$ if there were no forces and no friction. The force $\bar{\mathbf{F}}(t)$ is the combination of the forces derived from the Hamiltonian computed at time t and a random force which represents η_i . We choose a time step $\Delta=0.04$, which is about $\frac{1}{5}$ of the inverse of the maximum vibrational frequency $\omega_{\text{max}}=2\sqrt{2}$.

In order to save computer time, we actually use the random force and damping only on every eighth time step. Also, rather than using a random force with a Gaussian distribution, we employ a rectangular distribution with the correct second moment. Because the coupling to the heat bath is very weak, this should be a valid procedure. The random number generator employed has a cycle time much longer than the number of times it is called in our calculations.

We now describe the fit. The static correlation function $S(k)$ is fitted first by assuming Eqs. (6) and (8), and choosing a value for B_f and a range of the Brillouin zone over which the fit is performed. The correlation length ξ is extracted by minimizing the χ^2 with $S(k=0)$ and ξ for fitting parameters. The weights $\sigma(S(k))$ in the χ^2 are given by the statistical rms fluctuation of $S(k)$ over different runs. The scaling formula (6) used

is only valid for small kb ; therefore, one must choose a range of k to perform the fit. We found that when the range was changed from $[0, \pi/4]$ to $[0, \pi/8]$, this led only to a change of order 1% or less in the value of ξ (for a reasonable value of B_f). For a given B_f , one obtains ξ and $S(k=0)$ as a function of temperature and Eqs. (3) and (7) give a value for B_ξ and B_S for each temperature. The "best" choice of B_f gives the smallest variation in B_ξ and B_S ; the values obtained should then be consistent with (9). For the best fit ($B_f=0.10$, $B_S=125$, and $B_\xi=0.0100$) the formula (3) is equal to the fitted value of ξ within 2% for four temperatures from $[T=0.614, \xi=25.5b]$ to $[T=0.692, \xi=9.2b]$, while $S(k=0)$ as is given by (7) is equal to the fitted value within 5% in the same temperature range, and (9) is satisfied within 2%.

The dynamical correlation function is then fitted with (10) by minimizing the χ^2 at each temperature. Equations (11) and (12) contain more parameters than are actually necessary to fit our data within the accuracy of the calculations; we can proceed in two different ways. First one can adjust (11) to fit the location of the spin-wave peak at large k , which gives a value of $\delta \approx 1.7$. We then can do a best fit over the other parameters and get $\gamma_0=0.80$, $\mu=2.0$, and $\theta=0.15$. Alternatively, we can let all four parameters be free and minimize the χ^2 ; we then get $\delta=1.05$, $\gamma_0=0.86$, $\mu=1.4$, and $\theta=0.08$. The value for γ_0 which determines the relaxation rate at $k=0$ does not change much from one fit to the other, and we estimate the correct value as $\gamma_0=0.85 \pm 0.15$. This value appears to be very close to the value obtained by Grempe in his coupled-mode approximation⁴ (Grempe predicts $\gamma_0 \approx 0.96$). By contrast, the approximation of Auerbach and Arovas⁸ gives a characteristic frequency whose temperature dependence differs from our Eq. (2),

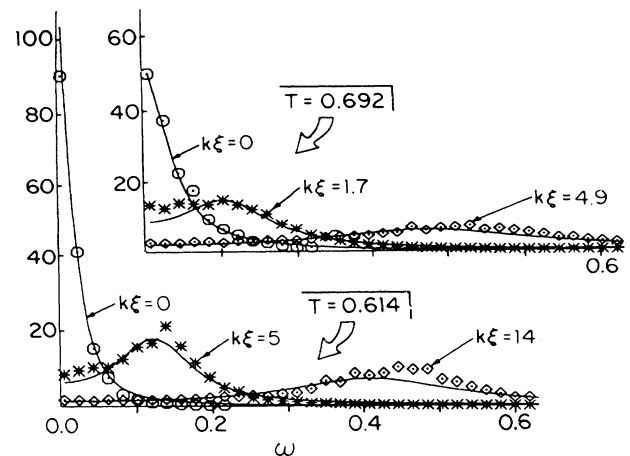


FIG. 1. The ratio $S(k, \omega)/S(k)$ plotted for three different values of k [$kb=0, 0.196$, and 0.557 in the $(0,1)$ direction] and two different temperatures ($T=0.614$ and 0.692). The data are represented by points, and the solid curves show our fit with parameters $\delta=1.05$, $\gamma_0=0.86$, $\mu=1.4$, $\theta=0.08$; values of $k\xi$ are indicated.

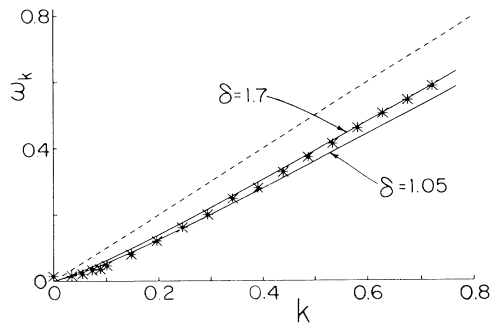


FIG. 2. The zero-temperature spin-wave frequency (dashed curve) compared to the scaling frequencies at $T=0.614$ for $\delta=1.7$ and $\delta=1.05$ (solid curves) and to the points obtained from a best fit of our data by the sum of two Lorentzians.

and a line shape which seems quite different from ours.

Our data for $S(k, \omega)/S(k)$ are shown in Fig. 1, at three values of k , for temperatures $T=0.614$ and $T=0.692$. The solid curves are the fit with $\delta=1.05$. The correlation lengths, in units of the lattice spacing, are $\xi=25.5$ and $\xi=9.2$ while $\bar{\omega}_0=0.0125$ and $\bar{\omega}_0=0.0368$ at the two temperatures. The broadening due to our use of a finite external damping constant $\gamma=0.00625$ is important primarily for $k=0$ at the lowest temperature. One qualitative difference between the data and our two-Lorentzian fit is that for intermediate values of $k\xi$, the data have more weight near $\omega=0$. Thus $S(k, \omega)$ has a maximum at $\omega \neq 0$ only for $q \gtrsim 2$, while for our fitted form this occurs as soon as $v_q > 3^{-1/2} \gamma_q$ —roughly for $q \gtrsim \frac{1}{2}$. The added weight at small ω depletes the higher- ω region and consequently the fitted form for $\Phi(q, \nu)$ is always greater than the data for $\nu \gg v_q$.

In Fig. 2, we show data for the spin-wave frequency ω_k for various values of k , at $T=0.614$, obtained by fitting $S(k, \omega)$ by the sum of the two Lorentzians. The solid curves are the predictions of Eq. (11) with $\delta=1.7$ and $\delta=1.05$ as indicated. The dashed curve is the spin-wave frequency at $T=0$. The net reduction in ω_k for $T \neq 0$ is interpreted as arising from a combination of a reduction in the effective spin stiffness (which reduces ω_k by a factor of ≈ 0.65 , at $k=0.6$) and the factor $(\frac{3}{2})^{1/2}$ in Eq. (11) which increases ω_k and arises from the difference between $\chi_{\perp}(T)$ and χ_{\perp}^0 .²

The scaling and renormalization-group analysis used in this paper is valid, in principle, in the limit $T \rightarrow 0$, for fixed arbitrary value of the product $k\xi$. In practice, we expect that the necessary condition on temperature is that ξ be large compared to the lattice constant. For this to occur in the classical model it is necessary that

$2\pi\rho_s/T \gtrsim 6$. For the $S = \frac{1}{2}$ QAFM, however, this only requires that $2\pi\rho_s/T \gtrsim 2$. Indeed, the asymptotic forms (5) and (7), with the parameter values predicted by our analysis, agree remarkably well with quantum Monte Carlo results for the QHAF⁹ for $2\pi\rho_s/T \approx 2$. For $S(k)$, the expected restrictions on wave vectors are $k \lesssim \pi/2b$ for the CLRM and $k \ll T/\hbar c$ for the QHAF. For $S(k, \omega)$ there is an additional restriction which for the QHAF is roughly of the form $ka \lesssim (a/\xi)^{0.2}$ (cf., Appendix D of CHN). For larger values of k , the factor $(\frac{3}{2})^{1/2}$ in the spin-wave frequency, Eq. (11), should be replaced by a factor $[\chi_{\perp}^0/\chi_{\perp}(T, k)]^{1/2}$, which tends to unity for large values of k .

If one desires to extend the formulas to the quantum region $k \approx T/\hbar c$, one should include on the right-hand side of Eqs. (6) and (1) additional factors, respectively, of $x \coth x$ and $\omega/[T(e^{\omega/T} - 1)x \coth x]$, where $x \equiv \hbar ck/2T$.

The authors are grateful for helpful conversations with R. Morf, R. Birgeneau, and especially D. R. Nelson. This work has been supported in part by the NSF through Grants No. DMR 88-17291 and No. DMR 86-01908, and the Harvard Materials Research Laboratory. Computations were performed on a Cyber 205 at the John von Neumann Computer Center.

(a)Permanent address: Physics Department, University of California at Los Angeles, Los Angeles, CA 90024.

¹Y. Endoh, K. Yamada, R. J. Birgeneau, D. R. Gabbe, H. P. Jenssen, M. A. Kastner, C. J. Peters, P. J. Picone, T. R. Thurston, J. M. Tranquada, G. Shirane, Y. Hidaka, M. Oda, Y. Enomoto, M. Susuki, and T. Murakami, Phys. Rev. B **37**, 7443 (1988).

²S. Chakravarty, B. Halperin, and D. Nelson, Phys. Rev. B (to be published).

³T. Oguchi, Phys. Rev. **117**, 117 (1960).

⁴D. R. Grempel, Phys. Rev. Lett. **61**, 1041 (1988).

⁵S. H. Shenker and J. Tobochnik, Phys. Rev. B **13**, 1299 (1976); see also M. Fukugita and Y. Oyanagi, Phys. Lett. **123B**, 71 (1983); S. Itoh, Y. Iwasaki, and T. Yoshié, Nucl. Phys. **B250**, 312 (1985).

⁶A. B. Harris, D. Kumar, B. I. Halperin, and P. C. Hohenberg, Phys. Rev. B **3**, 1299 (1976).

⁷R. Morf and E. Stoll, in *Numerical Analysis*, edited by J. Descloux and J. Marti (Birkhäuser, Basel, 1977); see also T. Schneider and E. Stoll, Phys. Rev. B **17**, 1302 (1978).

⁸A. Auerbach and D. Arovos, Phys. Rev. Lett. **61**, 617 (1988).

⁹G. Gomez-Santos, J. D. Joannopoulos, and J. W. Negele, Phys. Rev. B (to be published). Also, cf. E. Manousakis and R. Salvador, Phys. Rev. Lett. **60**, 840 (1988).